Scaling behaviour of dN/dy in high energy collisions

G. Kasza[1,2] and T. Csörgő[1,2],

[1] HUN-REN Wigner RCP, H-1525 Budapest, P.O.Box 49, Hungary
[2] MATE Institute of Technology KRC, H-3200 Gyöngyös, Mátrai út 36, Hungary

November 30, 2023

Abstract

From a recently found family of analytic, finite and accelerating, 1+1 dimensional solutions of perfect fluid relativistic hydrodynamics, we derive simple and powerful formulae to describe the rapidity and pseudorapidity density distributions. By introducing a new scaling function, we noticed that the rapidity distribution data of the different experiments are collapse into a single curve. This data collapsing behaviour of rapidity distributions suggests that high energy $p+p$ collisions may be described as collective systems.

1 Introduction

The Hwa-Bjorken solution of relativistic hydrodynamics is suitable for describing 1+1 dimensional explosive perfect fluids [1, 2]. The solution utilizes a time-independent Hubble-type velocity field, so one of its main shortcomings is that it assumes acceleration-free expansion. Consequently, it predicts a rapidity plateaux, or a flat rapidity distribution,

which does not describe any of the high energy experimental data at RHIC or LHC energies (except perhaps in a narrow interval near midrapidity, where the distribution is approximately constant near its maximum). However, one of the great advantages of this Hwa-Bjorken solution is that it uses simple formulas, and from this solution Bjorken derived his famous formula for estimating the initial energy density of the hot and dense matter created in heavy ion collisions [2]. This solution has previously been generalised to the case of an accelerating velocity field [3, 4], but these generalisations only satisfy the equations of hydrodynamics under strong constraints. In one of these new exact solutions [3, 4] the rate of acceleration may have an arbitrary constant value, but only for a superhard, non-realistic equation of state, where the speed of sound and the speed of light are equal. Recently, Csörgő, Kasza, Csanád and Jiang published a 1+1 dimensional generalization of the Hwa-Bjorken solution, where the rate of acceleration of the velocity field may have an arbitrary constant value, even for a realistic equations of state [5], referred to as the CKCJ solution.

This CKCJ family of perfect fluid solutions and its applications have been published previously. The calculation of the pseudorapidity distribution and the fitting of the resulting formula to experimental data were published in refs. [5, 6, 7]. The correction to Bjorken's initial energy density estimate was presented in detail in ref. [8]. Based on measured data, we have determined the lifetime parameter of heavy ion collisions for $\sqrt{s_{NN}} = 130$ and 200 GeV $Au + Au$ reactions and published the result in refs. [7, 9]. We calculated the initial energy density in $\sqrt{s_{NN}} = 130$ and 200 GeV $Au + Au$ collisions, which was also published in [7]. The most recent result is the evaluation of the thermal photon spectrum, which we compared with experimental data in ref. [10].

In this manuscript we show that, using a new formula computed from the solution reported in ref. [5], we find a data collapsing or scaling behaviour of experimental rapidity distribution data. This observation is one of the manifestations of a beautiful hydrodynamic scaling behaviour. Our theoretical insight is cross-checked on experimental data successfully, as shown explicitly in Section 4.

2 Recapitulation of the CKCJ Solution

In this section, we briefly recapitulate the 1+1 dimensional, analytical, accelerating family of CKCJ solutions of relativistic perfect fluid hydrodynamics from ref. [5]. The solutions of this family solve the equations of hydrodynamics at zero chemical potential ($\mu = 0$) under the following equation of state:

$$\varepsilon = \kappa_0 p, \tag{1}$$

where κ_0 is the inverse square of the speed of sound: $\kappa_0 = c_s^{-2}$, assumed to be a constant for simplicity. For the velocity field, the CKCJ generalization of the Hwa-Bjorken flow that allows the description of accelerating fluids reads as follows [5]:

$$u^\mu = (\cosh(\Omega), \sinh(\Omega)), \tag{2}$$

where Ω is the fluid-rapidity, which is the function of the coordinate-rapidity η_z, but it is independent from the longitudinal proper time τ (i.e. $\Omega \equiv \Omega(\eta_z)$). [5] The new family of CKCJ solutions [5] can be summarized as follows:

$$\begin{aligned}
\eta_z(H) &= \Omega(H) - H, && (3)\\
\Omega(H) &= \frac{\lambda}{\sqrt{\lambda-1}\sqrt{\kappa_0-\lambda}} \arctan\left(\sqrt{\frac{\kappa_0-\lambda}{\lambda-1}}\tanh(H)\right), && (4)\\
\sigma(\tau,H) &= \sigma_0\left(\frac{\tau_0}{\tau}\right)^{\lambda} \mathcal{V}(s)\left[1+\frac{\kappa_0-1}{\lambda-1}\sinh^2(H)\right]^{-\frac{\lambda}{2}}, && (5)\\
T(\tau,H) &= T_0\left(\frac{\tau_0}{\tau}\right)^{\frac{\lambda}{\kappa_0}} \mathcal{T}(s)\left[1+\frac{\kappa_0-1}{\lambda-1}\sinh^2(H)\right]^{-\frac{\lambda}{2\kappa_0}}, && (6)\\
\mathcal{T}(s) &= \frac{1}{\mathcal{V}(s)}, && (7)\\
s(\tau,H) &= \left(\frac{\tau_0}{\tau}\right)^{\lambda-1} \sinh(H)\left[1+\frac{\kappa_0-1}{\lambda-1}\sinh^2(H)\right]^{-\lambda/2}, && (8)
\end{aligned}$$

where T is the temperature and σ stands for the entropy density. The trajectory equation of the fluid element is defined by the scale variable s satisfying the scale equation $u^\mu \partial_\mu s = 0$. The function $\mathcal{T}(s)$ is an arbitrary function of the scale variable s. The parameter λ is an integration constant, but it has an important physical meaning, since it determines the acceleration of the velocity field: for $\lambda > 1$ we talk about accelerating expansion, while for $0 < \lambda < 1$ we consider decelerating expansion.

The above equations can be considered as a parametric family of solutions in the sense that the coordinate-rapidity dependence of the thermodynamic quantities (T, σ, p, ε) and the elements of the velocity field (Ω, v_z) is given through the parameter $H = \Omega(\eta_z) - \eta_z$. [5]

It is important to note that the above equations define a finite family of solutions in terms of the coordinate rapidity, and the range of validity of the solutions is affected by the values of λ and κ_0. However, in the accelerationless limiting case $\lambda \to 1$, the width of the range of validity goes to infinity. [5] Thus for low accelerations, this family of solutions can be applied in the physical domain of high energy collisions and in the $\lambda \to 1$ limit, the Hwa-Bjorken solution is recovered.

3 Evaluation of the rapidity density

The Cooper-Frye formula can be used to calculate the rapidity distribution:

$$\frac{dN}{dy} = \frac{1}{2\pi\hbar}\int d\Sigma_\mu p^\mu \exp\left(-\frac{p_\mu u^\mu}{T_{\mathrm{F}}\left(\tau_{\mathrm{f}},\eta_z\right)}\right), \tag{9}$$

where $d\Sigma_\mu$ is the normal vector of the freeze-out hypersurface, while p^μ is the four-momentum of the detected particles. The integral is performed on the freeze-out hypersurface, which is the set of points in spacetime (τ,η_z) where the hadronic medium is freezing-out. This integral is evaluated at vanishing chemical potential, thus the fugacity yields a trivial factor of unity in the Boltzmann integral, where T_{F} is the temperature of the freeze-out hypersurface, which is not a constant, since the points of the freeze-out hypersurface have different temperatures. The proper time associated with the freeze-out is denoted by τ_{f}. For the temperature, we use eq. (6), and we consider the simplest possible case, i.e., when the scale function is chosen to be unity: $\mathcal{T}(s) = 1$.

The new solution was found in 1+1 dimensional spacetime, so we had to embed the formula for the rapidity distribution in 1+3 dimensional spacetime. To do this, we first assumed that the temperature of the medium is homogeneous in the transverse plane, and thus the rapidity density is independent of the transverse coordinates. As a second step, we introduced the transverse mass m_{T} instead of the particle mass m. In such a case, the integration of the distribution on the surface perpendicular to the beam direction can be performed trivially, but the integration on the momentum space must also be performed. Turning to the transverse mass as an integration variable, the rapidity distribution embedded in the 3-dimensional space can be obtained by integrating the double-differential spectrum over the transverse mass. We used saddle point approximation in the calculations, which led to the following result:

$$\frac{dN}{dy} \approx \left.\frac{dN}{dy}\right|_{y=0} \cosh^{-\frac{\alpha(\kappa_0)}{2}-1}\left(\frac{y}{\alpha}\right) \exp\left(-\frac{m}{T_{\mathrm{f}}}\left[\cosh^{\alpha(\kappa_0)}\left(\frac{y}{\alpha}\right)-1\right]\right), \tag{10}$$

where $\alpha(\kappa_0) = (2\lambda-\kappa_0)/(\lambda-\kappa)$, and $\alpha(1) = \alpha$. The kinetic freeze-out temperature is denoted by T_{f} and y stands for the rapidity.

In eq. (10) the contribution of radial flow is not present, but from the p_{T}-spectra it is known that the radial flow effect is not negligible. While the embedding of the rapidity distribution in 3 spatial dimensions is an efficient tool, it makes the assumption that the temperature is homogeneous in the transverse plane. For this reason, the effect of radial flow does not appear, so we artificially include it in the equations. We introduce the effective temperature T_{eff}, which is equal to the sum of the kinetic freeze-out temperature T_{f} and the contribution of the radial flow. In the formula for the rapidity distribution, we simply use the notation $T_{\mathrm{f}} \to T_{\mathrm{eff}}$ to sneak the radial flow contribution into the distribution [5,

6]:

$$\frac{dN}{dy} \approx \left.\frac{dN}{dy}\right|_{y=0} \cosh^{-\frac{\alpha(\kappa_0)}{2}-1}\left(\frac{y}{\alpha}\right) \exp\left(-\frac{m}{T_{\rm eff}}\left[\cosh^{\alpha(\kappa_0)}\left(\frac{y}{\alpha}\right)-1\right]\right). \tag{11}$$

The midrapidity density can be expressed by the following formulae:

$$\left.\frac{dN}{dy}\right|_{y=0} = \frac{1}{\sqrt{\lambda(2\lambda-1)}} \frac{V_x V_p}{(2\pi\hbar)^3} \exp\left(-\frac{m}{T_{\rm eff}}\right), \tag{12}$$

$$V_x = R^2 \pi \tau_{\rm f}, \tag{13}$$

$$V_p = (2\pi m T_{\rm eff})^{3/2}. \tag{14}$$

Here, $R^2\pi$ is the finite size of the transverse plane, V_x is the volume of the coordinate space, and V_p is the volume of the momentum space. While the midrapidity density depends on several parameters of the model, for simplicity we will now consider it only as a normalization constant, which will greatly facilitate the fitting of experimental data.

3.1 The approximate formula for the rapidity distribution

We now summarize in a few lines that further approximations can be made on eq. (11) of the rapidity distribution in the region where $|y| \ll \alpha = 2 + 1/(\lambda - 1)$. Obviously, this region widens rapidly if one goes to the accelerationless limiting case ($\lambda \to 1$). In this approximation, the rapidity distribution becomes a Gaussian distribution [7]:

$$\frac{dN}{dy} \approx \frac{\langle N \rangle}{(2\pi\Delta y^2)^{1/2}} \exp\left(-\frac{y^2}{2\Delta y^2}\right). \tag{15}$$

In this approximation, the two new parameters are the average multiplicity $\langle N \rangle$ and Δy, which characterizes the width of the distribution. Both quantities can be expressed in terms of the parameters of the rapidity density embedded in the 3-dimensional space [7]:

$$\frac{1}{\Delta y^2} = (\lambda-1)^2 \left[1 + \left(1 + \frac{1}{\kappa_0}\right)\left(\frac{1}{2} + \frac{m}{T_{\rm eff}}\right)\right], \tag{16}$$

$$\langle N \rangle = \left(2\pi\Delta y^2\right)^{1/2} \left.\frac{dN}{dy}\right|_{y=0}. \tag{17}$$

Such a Gaussian rapidity distribution is by no means a unique result that is characteristic to the CKCJ solution only. Other calculations and model results, that are based on Landau hydrodynamics usually predict a similar result, see e.g. refs. [11, 12, 13]. Using eq. (15), the experimental data can be described by fitting two parameters ($\langle N \rangle$ and Δy), while the original formula (11) has four parameters to be fitted (κ_0, λ, $T_{\rm eff}$, $dN/dy|_{y=0}$). This result is a wonderful manifestation of hydrodynamic scaling behavior: two different fits of the data, resulting in different parameter sets, can lead to the same curve, provided that the values of the two relevant combinations of the four original parameters, (16) and (17), remain the same. From eq. (15) of the rapidity distribution, it is also clear that the

rapidity density can be normalized by both the midrapidity value of the distribution and the mean multiplicity.

3.2 The approximate formula for the pseudorapidity distribution

The pseudorapidity distribution can be calculated from the double-differential invariant momentum spectrum and can be written as the product of two factors. One is the rapidity density, which written in eq. (11). The other factor is the Jacobian determinant $\mathcal{J}$, calculated for a mean rapidity dependent transverse momentum: $\langle p_{\mathrm{T}}(y)\rangle$. [7]

The pseudorapidity distribution and the partial results of its derivation were described in details in ref. [7], so we will leave it aside for now. In this manuscript, we focus on an approximate formula that holds in the limiting case $\lambda \to 1$. In this case, the Jacobi determinant and the pseudorapidity distribution can be approximated by the following equations [7]:

$$\mathcal{J} \approx \frac{\cosh(\eta_{\mathrm{p}})}{\sqrt{D^2 + \cosh^2(\eta_{\mathrm{p}})}}, \tag{18}$$

$$\frac{dN}{d\eta_{\mathrm{p}}} \approx \frac{\langle N\rangle}{\sqrt{2\pi\Delta y^2}} \frac{\cosh(\eta_{\mathrm{p}})}{\sqrt{D^2 + \cosh^2(\eta_{\mathrm{p}})}} \exp\left(-\frac{y^2\left(\eta_{\mathrm{p}}\right)}{2\Delta y^2}\right), \tag{19}$$

where η_p is the pseudorapidity, $D = m/\langle p_{\mathrm{T}}\rangle$ stands for the depthness-parameter. In eq. (19), the $y(\eta_{\mathrm{p}})$ rapidity can be approximated as follows [7]:

$$y(\eta_{\mathrm{p}}) \approx \tanh^{-1}\left(\frac{\cosh(\eta_{\mathrm{p}})}{\sqrt{D^2 + \cosh^2(\eta_{\mathrm{p}})}} \tanh\left(\eta_{\mathrm{p}}\right)\right). \tag{20}$$

4 The scaling of dN/dy data

The Gaussian density is expressed by (15) and is determined by the normalization factor and the width of the distribution. These parameters thus carry the characteristics of the different reactions, such as the collision energy, the size of the colliding system and the centrality of the collision. The normalization factor and the width of the distribution can be scaled out from eq. (15), and with that we obtain a curve independent from the characteristics of the reactions. We introduce the variable x, which is the quotient of the rapidity y and the width Δy:

$$x = \frac{y}{\Delta y}. \tag{21}$$

Then we divide the rapidity distribution by the normalization factor, introducing a scale-independent distribution:

$$\left(\left.\frac{dN}{dy}\right|_{y=0}\right)^{-1} \frac{dN}{dy} = \exp\left(-\frac{x^2}{2}\right), \tag{22}$$

where the expression of the normalization factor is given by eq. (17), which is valid in the $|y| \ll \alpha$ range. Our idea is that if we scale back the rapidity distribution data from different reactions with the normalization factor and Δy as above, then regardless of the reaction, all the data series will line up on the curve of eq. (22). However, in most cases, we do not have dN/dy measurements available, so in order to check our conjecture, we have transformed the available pseudorapidity density data. For this reason, first we used eq. (19) to determine the parameters D, $\langle N \rangle$ and Δy from the pseudorapidity distribution data. Thus, for each dataset we obtained different values of D, $\langle N \rangle$ and Δy. Using the D parameter, we could determine the Jacobian determinant to transform the pseudorapidity distribution data points into rapidity distribution data points. Then the mean multiplicity $\langle N \rangle$ and the width parameter Δy were used to rescale the rapidity distributions. Thus this scale function can be written as:

$$f(x) = \exp(-x^2/2). \tag{23}$$

Using this method, we checked the manifestation of the scaling behavior on eleven data sets: PHOBOS 0-30% $Au + Au$ at $\sqrt{s_{NN}} = 20$, 62.4, 130 [14], CMS $p + p$ at $\sqrt{s} = 7$, 8 and 13 TeV and 0-80% $Xe + Xe$ at $\sqrt{s_{NN}} = 5.44$ TeV [15, 16, 17, 18], and ALICE $Pb + Pb$ at $\sqrt{s_{NN}} = 5.02$ TeV for central, mid-central and peripheral collisions [19]. A comparison of these data with eq. (22) is shown in Fig. 1. The vertical errors of the data points consist of the statistical errors of the pseudorapidity distributions and the uncertainty of the Jacobian determinants. For the PHOBOS data we had to use a special method, as PHOBOS did not publish separately the statistical and systematic errors of the pseudorapidity distributions. For this reason, we used an estimate for the statistical errors of the PHOBOS data, which is described in detail in ref. [7]. The horizontal error of the data points is due to the uncertainty of Δy. Fig. 1 convincingly illustrates that our conjecture was right, i.e. all the data points measured in the different reactions are clustered within error on the blue curve, which is the manifestation of hydrodynamic scaling behaviour in the experimental data.

For the pseudorapidity distributions, we could not find a scale function similar to eq. (23) to describe the collapse of the experimental datasets of $dN/d\eta_{\rm p}$, as we saw for the rapidity distributions in Fig. 1. It is due to the appearance of the depth parameter D, which controls the dip of the pseudorapidity distribution around midrapidity. This can be easily seen by evaluating eq. (19) in zero pseudorapidity:

$$\left.\frac{dN}{d\eta_{\rm p}}\right|_{\eta_{\rm p}=0} = \left.\frac{dN}{dy}\right|_{y=0} \frac{1}{\sqrt{1+D^2}}, \tag{24}$$

where we used eq. (17) for the midrapidity density. Thus, if this dip is close to zero ($D \approx 0$),

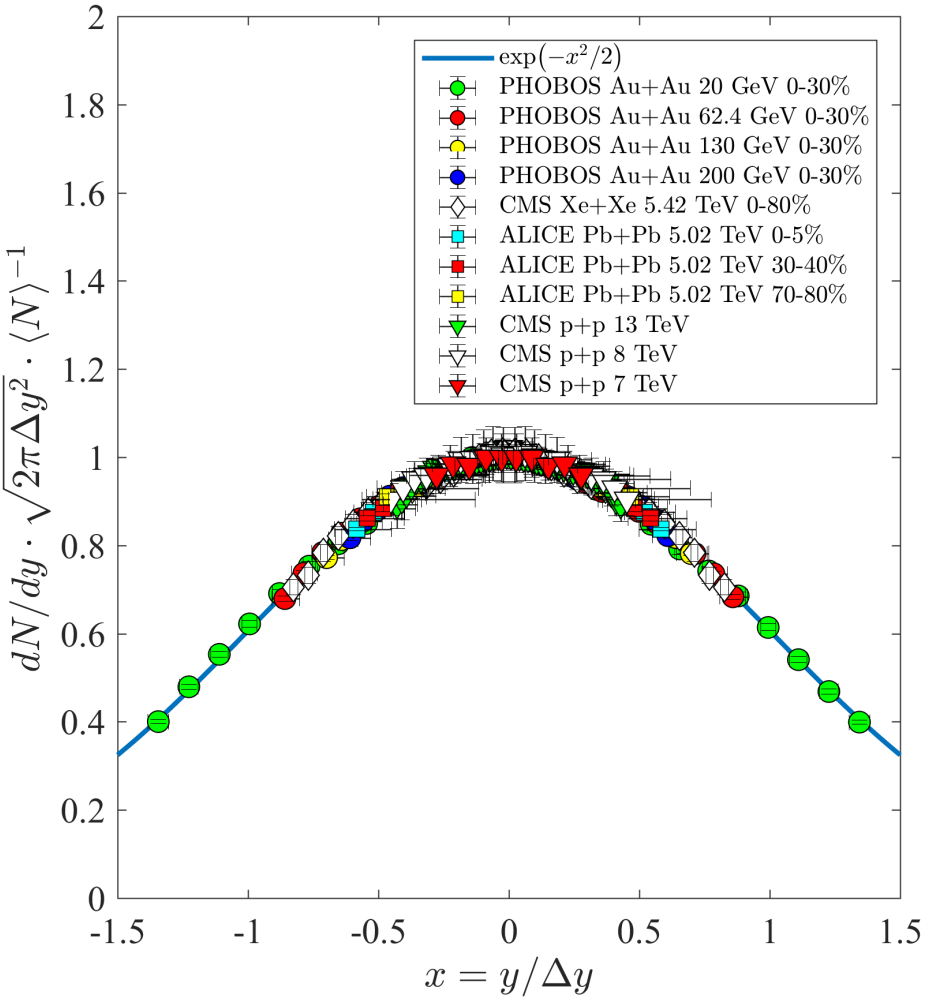

Figure 1: Manifestation of hydrodynamic scaling behaviour on experimental data: by transforming the pseudorapidity distributions measured in different reactions, we calculated the data points associated with the rapidity densities, which we rescaled by the normalization factor. The width of the distributions were also scaled out by introducing the variable x. All of the resulting data points lie within error on the scale independent blue curve obtained from our theoretical calculations. The datasets were taken from CMS [15, 16, 17, 18], ALICE [19] and PHOBOS [14].

we recover the formula of the rapidity distribution and the scaling behavior is restored. This phenomenon is illustrated in Fig. 2.

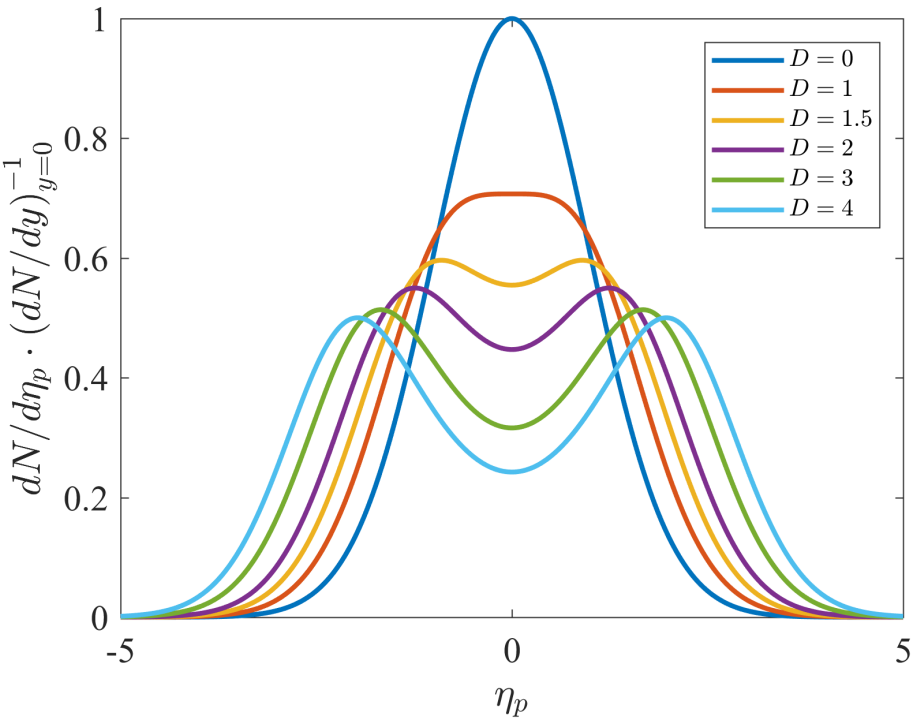

Figure 2: The pseudorapidity distribution (divided by $dN/dy|_{y=0}$) for different D values. The width parameter Δy is fixed to 1. It can be clearly seen that the closer D approaches 0, the smaller the midrapidity dip of the pseudorapidity distribution, and for $D = 0$, we recover eq. (15) for the shape of the rapidity distribution.

5 Conclusions

In this manuscript, we introduced a new approximate formula to describe the rapidity distributions, based on the solution published in ref. [5]. By rescaling the new formula, we introduced a new scale function to show the data collapsing of the rapidity distribution measurements. This data collapsing behaviour was tested on 11 datasets from three different experiments (CMS, PHOBOS, ALICE). It is important to emphasize that these datasets are not only from nucleus-nucleus collisions, but also from proton-proton collisions, which are also described by the curve of the scale function. From this result we can conclude that $p+p$ collisions can also be treated as collective systems, as far as their rapidity or pseudo-rapidity distributions are concerned. Let us mention, that the $p+p$ data can be well described with low speed of sound values ($c_s^2 = 0.1$), which is typical for fluids. This suggests that a strongly interacting quark-gluon plasma my be formed in $p+p$ collisions at RHIC and at LHC energies.

Let us emphasize that the hydrodynamical description of small systems (hadron-hadron

collisions) is not a new idea. The EHS/NA22 collaboration previously estimated some hydrodynamic model parameters (radial flow, kinetic freeze-out temperature, geometric radius of the particle source, mean lifetime) via invariant momentum distributions of π^- particles and Bose-Einstein correlation functions in $(\pi^+/K^+)p$ reactions at $\sqrt{s} \approx 22$ GeV, where the mean multiplicity of charged particles was less then 10. [20]

Acknowledgements

This research has been partially supported by NKFIH K-133046, NKFIH K-147557 and MATE KKP (2023) grants.

References

[1] R. C. Hwa. "Statistical Description of Hadron Constituents as a Basis for the Fluid Model of High-Energy Collisions". In: *Phys. Rev. D* 10 (1974), p. 2260. DOI: 10.1103/PhysRevD.10.2260.

[2] J. D. Bjorken. "Highly Relativistic Nucleus-Nucleus Collisions: The Central Rapidity Region". In: *Phys. Rev. D* 27 (1983), pp. 140–151. DOI: 10.1103/PhysRevD.27.140.

[3] T. Csörgő, M. I. Nagy, and M. Csanád. "A New family of simple solutions of perfect fluid hydrodynamics". In: *Phys. Lett. B* 663 (2008), pp. 306–311. DOI: 10.1016/j.physletb.2008.04.038. arXiv: nucl-th/0605070.

[4] M. I. Nagy, T. Csörgő, and M. Csanád. "Detailed description of accelerating, simple solutions of relativistic perfect fluid hydrodynamics". In: *Phys. Rev. C* 77 (2008), p. 024908. DOI: 10.1103/PhysRevC.77.024908. arXiv: 0709.3677 [nucl-th].

[5] T. Csörgő et al. "New exact solutions of relativistic hydrodynamics for longitudinally expanding fireballs". In: *Universe* 4.6 (2018), p. 69. DOI: 10.3390/universe4060069. arXiv: 1805.01427 [nucl-th].

[6] T. Csörgő et al. "A new and finite family of solutions of hydrodynamics. Part I: Fits to pseudorapidity distributions". In: *Acta Phys. Polon. B* 50 (2019), pp. 27–35. DOI: 10.5506/APhysPolB.50.27. arXiv: 1806.06794 [nucl-th].

[7] G. Kasza and T. Csörgő. "Lifetime estimations from RHIC Au+Au data". In: *Int. J. Mod. Phys. A* 34.26 (2019), p. 1950147. DOI: 10.1142/S0217751X19501471. arXiv: 1811.09990 [nucl-th].

[8] G. Kasza and T. Csörgő. "A new and finite family of solutions of hydrodynamics: Part II: Advanced estimate of initial energy densities". In: *13th Workshop on Particle Correlations and Femtoscopy*. June 2018. DOI: 10.5506/APhysPolBSupp.12.175. arXiv: 1806.11309 [nucl-th].

[9] T. Csörgő and G. Kasza. "A new and finite family of solutions of hydrodynamics: Part III: Advanced estimate of the life-time parameter". In: (Sept. 2018). DOI: 10.5506/APhysPolBSupp.12.217. arXiv: 1810.00154 [nucl-th].

[10] G. Kasza. "Describing the thermal radiation in $Au + Au$ collisions at $\sqrt{s_{NN}}$ =200 GeV by an analytic solution of relativistic hydrodynamics". In: (Nov. 2023). arXiv: 2311.03568 [nucl-th].

[11] C-Y. Wong. "Landau Hydrodynamics Revisited". In: *Phys. Rev. C* 78 (2008), p. 054902. DOI: 10.1103/PhysRevC.78.054902. arXiv: 0808.1294 [hep-ph].

[12] C-Y. Wong et al. "Analytical Solutions of Landau (1+1)-Dimensional Hydrodynamics". In: *Phys. Rev. C* 90.6 (2014), p. 064907. DOI: 10.1103/PhysRevC.90.064907. arXiv: 1408.3343 [nucl-th].

[13] A. Sen et al. "Hydrodynamics from Landau initial conditions". In: *J. Phys. Conf. Ser.* 630.1 (2015), p. 012042. DOI: 10.1088/1742-6596/630/1/012042.

[14] B. Alver et al. "Phobos results on charged particle multiplicity and pseudorapidity distributions in Au+Au, Cu+Cu, d+Au, and p+p collisions at ultra-relativistic energies". In: *Phys. Rev. C* 83 (2011), p. 024913. DOI: 10.1103/PhysRevC.83.024913. arXiv: 1011.1940 [nucl-ex].

[15] V. Khachatryan et al. "Transverse-momentum and pseudorapidity distributions of charged hadrons in pp collisions at $\sqrt{s} = 7$ TeV". In: *Phys. Rev. Lett.* 105 (2010), p. 022002. DOI: 10.1103/PhysRevLett.105.022002. arXiv: 1005.3299 [hep-ex].

[16] S. Chatrchyan et al. "Measurement of pseudorapidity distributions of charged particles in proton-proton collisions at $\sqrt{s} = 8$ TeV by the CMS and TOTEM experiments". In: *Eur. Phys. J. C* 74.10 (2014), p. 3053. DOI: 10.1140/epjc/s10052-014-3053-6. arXiv: 1405.0722 [hep-ex].

[17] A. M. Sirunyan et al. "Measurement of charged pion, kaon, and proton production in proton-proton collisions at $\sqrt{s} = 13$ TeV". In: *Phys. Rev. D* 96.11 (2017), p. 112003. DOI: 10.1103/PhysRevD.96.112003. arXiv: 1706.10194 [hep-ex].

[18] A. M. Sirunyan et al. "Pseudorapidity distributions of charged hadrons in xenon-xenon collisions at $\sqrt{s_{\mathrm{NN}}} = 5.44$ TeV". In: *Phys. Lett. B* 799 (2019), p. 135049. DOI: 10.1016/j.physletb.2019.135049. arXiv: 1902.03603 [hep-ex].

[19] J. Adam et al. “Centrality dependence of the pseudorapidity density distribution for charged particles in Pb-Pb collisions at $\sqrt{s_{\mathrm{NN}}} = 5.02$ TeV”. In: *Phys. Lett. B* 772 (2017), pp. 567–577. DOI: 10.1016/j.physletb.2017.07.017. arXiv: 1612.08966 [nucl-ex].

[20] N. M. Agababyan et al. “Estimation of hydrodynamical model parameters from the invariant spectrum and the Bose-Einstein correlations of pi- mesons produced in (pi+ / K+)p interactions at 250-G V/c”. In: *Phys. Lett. B* 422 (1998), pp. 359–368. DOI: 10.1016/S0370-2693(98)00072-0. arXiv: hep-ex/9711009.